Eur. Phys. J. E **15**, 465–472 (2004)
DOI 10.1140/epje/i2004-10079-y

THE EUROPEAN PHYSICAL JOURNAL E

Spherical polyelectrolyte block copolymer micelles: Structural change in presence of monovalent salt

F. Muller[1,a], P. Guenoun[2,b], M. Delsanti[2], B. Demé[3], L. Auvray[4], J. Yang[5], and J.W. Mays[6]

[1] DRECAM, Service de Physique de l'Etat Condensé, CEA-Saclay, F-91191 Gif-sur-Yvette Cedex, France
[2] DRECAM, Laboratoire Interdisciplinaire sur l'Organisation Nanométrique et Supramoléculaire (LIONS), Service de Chimie Moléculaire, CEA-Saclay, F-91191 Gif-sur-Yvette Cedex, France
[3] Institut Laue-Langevin, B.P. 156, F-38042 Grenoble Cedex, France
[4] DRECAM, Laboratoire Léon Brillouin, CEA-Saclay, F-91191 Gif-sur-Yvette Cedex, France
[5] Waters Corporation, 34 Maple Street, Milford, MA 01757-3696, USA
[6] Department of Chemistry, University of Tennessee, Chemical Sciences Division, Oak Ridge National Laboratory, 552 Buehler Hall, Knoxville, TN 37996-1600, USA

Received 8 January 2004 and Received in final form 29 July 2004 /
Published online: 15 December 2004 –

Abstract. Spherical polyelectrolyte block copolymer micelles were investigated as a function of added NaCl salt concentration using Small-Angle Neutron Scattering (SANS) and Light Scattering (LS). The micelles are formed by the self-association of charged-neutral copolymers made of a long deuterated polyelectrolyte moiety $(NaPSS_d)_{251}$ and a short hydrophobic moiety $(PEP)_{52}$. In presence of salt, the core shape and the aggregation number of the micelles are not affected. The hydrodynamic radius of the micelle is found to be identical to the radius of the whole micelle deduced from neutron scattering and thus the hydrodynamic radius is a valid measure of the corona thickness. At the lowest salt concentrations investigated the thickness of the corona, R_s, remains essentially constant and a contraction is observed above an added-salt concentration c_s of 2×10^{-2} M where this crossover concentration corresponds to the average ionic strength of the free counterions in the corona. The contraction takes place while maintaining a rod-like behavior of the chains at short scale and obeys to: $R_s \sim c_s^{-0.18}$. The exponent 0.18 suggests an electrostatic persistence length proportional to the Debye screening length.

PACS. 61.25.Hq Macromolecular and polymer solutions; polymer melts; swelling – 82.35.Rs Polyelectrolytes – 83.80.Uv Block copolymers

1 Introduction

Polyelectrolyte brushes are attracting a lot of interest for many different applications. As shown recently [1], these brushes can act as more efficient lubricants than their neutral counterparts, probably because of the large number of counterions trapped within such charged brushes. From a biomimetic point of view, these charged brushes are also representative of some of the materials which cover cells, like glycocalyx layers or of components of the extra cellular matrix such as hyaluronic acid [2]. In addition, in spherical geometry, charged brushes may protect colloidal particles and be employed for drug delivery [3]. Many of these applications are relevant to salted media where one of the most exceptional features of charged polyelectrolyte brushes is a weak dependence of the brush extension on added salt. This has been predicted theoretically [4] and confirmed experimentally [5–8] to some extent. However, beyond this clear insensitivity, many questions remain unaddressed such as the real statistics of the chains when salt goes into the brush and the behavior of the persistence length of such charged chains which was found to be large in absence of salt [9]. Theory predicts distinct behaviors for flexible chains with a low density of charges [10] and for highly charged chains whose electrostatic stiffness must be taken into account [11].

In this work we make use of the insensitivity to salt of the aggregation number of micelles of charged-neutral diblock copolymers in order to examine spherical charged brushes whose surface density is fixed. This is shown in a first part thanks to neutron scattering on the micellar cores only. Our system, whose aggregation number is insensitive to salt addition, can mimick an assembly of fixed

[a] *Present address*: Department of Physics, Soft Condensed Matter Group, University of Fribourg, Chemin du Musée 3, CH-1700 Fribourg, Switzerland.
[b] e-mail: guenoun@drecam.saclay.cea.fr

spherical polyelectrolyte brushes whose conformation can be studied without any density change.

Then, in a second part, the brush extension at a fixed density is measured by coupled measurements of inelastic light scattering and neutron scattering. Comparison of the two kinds of measurements shows that the latter extension varies with added salt and is adequately characterized by the micelle hydrodynamic radius. The contraction of the charged shell only occurs above a salt threshold equal to the inner salt concentration of a micelle with no added salt, as already well established in the spherical case [6,7] by light scattering and in the planar case [8, 12] by force measurements or X-ray reflectivity. Above this threshold, the neutron scattering data at intermediate scattering vectors confirm the corona contraction [13,14] observed in cases of fixed [13] density of annealed chains or variable [14] surface density of quenched chains. These two latter examples seem to present complications due to phase separation within the corona. Our simpler case of fixed density of quenched chains enables to evidence a new feature: whereas the global contraction described by a single corona conformation is observed, at high scattering vectors values (local scale) the chains maintain a rigid conformation even at large salt concentrations. This result can be interpreted in term of a large persistence length l_p (of about 3 nm at a salinity of 3 M) whose evolution with added salt can be modeled through a scaling approach which balances the chain elasticity and a virial-like electrostatic interaction between segments. The contraction law we find is in agreement with a proportionality of l_p with the Debye screening length. Such an experimental result obtained in a configuration with a fixed density shows that a salted charged brush does not exactly contract by switching to the conformation of a neutral flexible brush in good solvent.

2 Experimental section

2.1 Materials

A diblock copolymer made of deuterated sodium poly(styrene sulfonate) ($NaPSS_d$) and of poly(ethylene-alt-propylene) (PEP) was used. The poly(styrene)/PEP diblock was synthesized by anionic polymerization [15]. This diblock is asymmetric (52 PEP units and 251 PS_d units) with a low index of polydispersity $M_w/M_n = 1.04$. The synthesis of the $NaPSS_d$/PEP diblock involved the sulfonation of the poly(styrene) component [15] and the extent of sulfonation, f, is found to be 90% as measured by elemental analysis.

The solvents used were de-ionized H_2O water (MilliQ Millipore system, 18 M$\Omega \cdot$cm) and/or pure D_2O with sodium chloride (Normapur grade, Prolabo Inc.).

2.2 Micellization of $(PEP)_{52}/(NaPSS_d)_{251}$ copolymer in salt-free solutions

In previous work [16], it has been shown that the copolymer chains form micelles composed of a small spherical core, formed by the association of the PEP moieties, having a radius $R_c = 4.5 \pm 0.1$ nm. The $NaPSS_d$ moieties are tethered to this core forming a large charged corona, having a radius $R_s = 33 \pm 3$ nm (R_s is defined as the whole radius of the micelle minus the core radius R_c). The aggregation number, *i.e.* the number of chains per micelle, was found to be $p = 54 \pm 4$. The overlap polymer concentration of the micelles was estimated to be $c^* \approx 2$ wt% in pure H_2O without salt.

2.3 Scattering experiments

For Small-Angle Neutron Scattering (SANS), the water used was pure D_2O or a mixture, D_2O 4 vol% in H_2O, which has a scattering length density identical to that of the $NaPSS_d$ or PEP groups, respectively. After addition of sodium chloride, the samples were transferred into quartz cells of inner thickness 2 mm and 1 mm for large salt concentration. The copolymer concentrations, c, were smaller than 1.5 wt%, which is below the overlap concentration of the micelles.

Experiments were performed at LLB at Saclay, on the PACE spectrometer [17], or at ILL (Grenoble) on the D22 spectrometer [18]. On the PACE spectrometer, wavelengths of 0.5 nm and 1 nm and sample-to-detector distances of 1.9 m and 4.7 m were used, respectively. A wavelength of 0.8 nm and sample-to-detector distances of 2 m and 17.6 m were used on the D22 spectrometer. We covered the scattering vector range $4 \times 10^{-2}\,\mathrm{nm}^{-1}$–$3 \times 10^{-1}$ nm^{-1} with PACE and $2 \times 10^{-2}\,\mathrm{nm}^{-1}$–1 nm^{-1} with the D22 spectrometer.

The scattered intensities were corrected for the parasitic intensity scattered by the cell and the scattering intensity of the solvent was subtracted using the standard procedure [16]. The remaining signal was normalized by the incoherent scattering of light water in order to convert the data into differential cross-sections per unit volume, $\sigma(\mathrm{cm}^{-1})$ and for convenience this quantity will be called sometimes "absolute scattered intensity". The signal obtained is mainly due to the coherent scattering, the incoherent scattering of the copolymer was found to be negligible both by calculation and measurements [19].

For Quasi-Elastic Light Scattering (QELS), very dilute samples ($c \leqslant 5 \times 10^{-2}$ wt%) were prepared with light water and then sodium chloride was added. Samples were filtered through 0.4 μm pore size filters (Nucleopore) directly into the scattering cell (13 mm inner diameter). QELS experiments were done using an Amtech goniometer SM200 and a Brookhaven correlator (BI2030AT). The light source was a vertically polarized beam (Argon laser, Coherent) of wavelength $\lambda = 514.5$ nm. The normalized time autocorrelation functions of the scattered electric field $g_1(t)$ were extracted from the autocorrelation functions of the intensity $\langle I(t)I(0)\rangle$: $g_1(t) = B[(\langle I(t)I(0)\rangle/\langle I^2\rangle) - 1]^{1/2}$, where B is a dimensionless factor which depends on the geometry of the experimental setup. The functions $g_1(t)$ were analyzed by the cumulant method in order to obtain the mean decay rate, Γ, of $g_1(t)$ [20]. Experiments were performed at scattering angles θ between 40 ° and 140 °. The

apparent diffusion coefficient, D_{app}, was deduced from Γ: $D_{app} = \Gamma/q^2$, where q is the scattering vector defined as $q = (4\pi n/\lambda)\sin(\theta/2)$ with n the refractive index of the solution. At small q-values, a strong q-dependence of D_{app} is found [21]. The diffusion coefficient of the micelles, D_m, was then determined using the values of D_{app} at high q-values ($\theta > 70\,^\circ$) and extrapolated to zero q-value according to the procedure previously described [21]. As the samples were very dilute, the hydrodynamic radii of the micelles R_h were deduced from D_m by use of the Stokes-Einstein law: $R_h = kT/6\eta D_m$ where η is the viscosity of the brine (H_2O plus NaCl). All the scattering experiments were performed at room temperature ($\approx 20\,^\circ$C).

3 Results and discussion

3.1 Core conformation and inter-structure factor of micelles

The core conformation was studied by neutron scattering on samples with pure D_2O (the $NaPSS_d$ groups are invisible in this way). The scattering curves obtained at a polymer concentration of $c = 1.33$ wt% ($c/c^* \approx 0.66$) for two different NaCl concentrations up to 2 M, are shown in Figure 1. At very small scattering vectors $q < 0.055$ nm^{-1}, regardless of the salt concentration, an excess of intensity is observed. At intermediate scattering vectors (0.055 nm^{-1}–0.2 nm^{-1}), the presence of peaks reflects that the signal is sensitive to the interactions between micelles. In salt-free solution, at high scattering vector $q > q^\dagger$ ($= 0.2\,\mathrm{nm}^{-1}$), the signal is directly proportional to the copolymer concentration when c is smaller than 1.9% [16] which means that, at the spatial scale q^{-1}, the interactions are negligible and the signal is directly proportional to the form factor of the cores. In this q range, Figure 1 unambiguously shows that the scattering curves in salt solutions are close to the one obtained in salt-free solution. The differential cross-sections per unit volume could be fitted by

$$\sigma(q > q^\dagger) = \sigma_c P_c(q)\,, \qquad (1)$$

where $P_c(q)$ is the form factor of a uniformly dense sphere of radius R_c:

$$P_c(q) = \{[3/(qR_c)^3] \cdot [\sin(qR_c) - qR_c\cos(qR_c)]\}^2\,. \qquad (2)$$

σ_c is the differential cross-section per unit volume of the cores without interactions at $q = 0$ which is proportional to the aggregation number of the micelle p:

$$\sigma_c = (c\rho/pM)b_c^2 N_c^2 p^2, \qquad (3)$$

where b_c is the apparent contrast length of the PEP monomer in the solvent, and N_c the degree of polymerization of the PEP moiety. The term in brackets represents the number density of micelles, where c is the copolymer concentration in g/g, ρ is the density of the solution, and M is the mass of the diblock chain (9.5×10^{-20} g). Such a form factor (Eqs. (1–3)) is reported in Figure 1

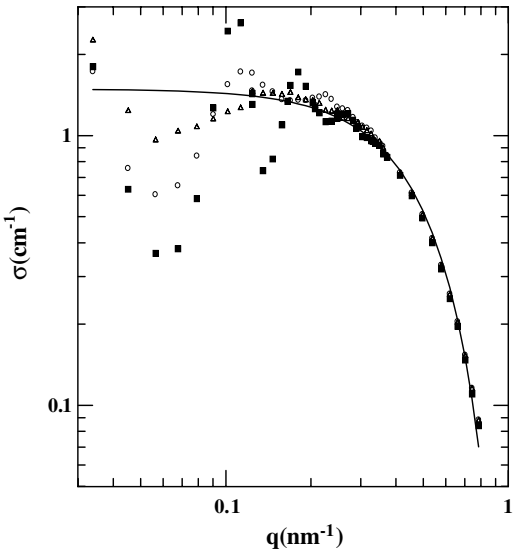

Fig. 1. Absolute intensity scattered by the cores of micelles *versus* scattering vector q measured on dilute samples ($c = c^*/1.5$) at different NaCl concentrations: $c_s = 1$ M (open triangles), $c_s = 0.1$ M (open circles), $c_s = 0$ M (full squares). The solvent used is D_2O which makes only the PEP group visible in neutron scattering experiment: at high scattering vectors, the signals reflect the form factor of the cores. The full line represents the differential cross-section per unit volume calculated from equations (1–3) with a sphere of radius $R_c = 4.5$ nm and an aggregation number of 54.

with $R_c = 4.5 \pm 0.1$ nm and $p = 54$ (which are the values found in salt-free solutions). It is clear that the core shape and the aggregation number are not affected by increasing the NaCl concentration. At this point, it is worth comparing our results with earlier measurements on diblocks $(PtBS)_{26}$-$(NaPSS)_{413}$ by P. Guenoun *et al.* [6], $(PS)_{20}$-$(PANa)_{80}$ by Van der Maarel *et al.* [13] and $(PEE)_{144}$-$(PSSH)_{136}$ by Förster *et al.* [14]. By comparing these latter measurements, the influence of salt on aggregation seems to be connected to the symmetry of the diblock copolymer. To characterize this symmetry, let us define β as the fraction of hydrophobic monomers in the diblocks. At high added-salt concentrations, the aggregation number was shown to decrease with c_s for a highly asymmetrical diblock ($\beta = 0.06$) [6], whereas it was shown to increase for a symmetrical diblock ($\beta = 0.5$) of $(PEE)_{144}$-$(PSSH)_{136}$. At an intermediate β-value (≈ 0.2), the present results and the data by Van der Maarel *et al.* [13] on the $(PS)_{20}$-$(PANa)_{80}$ diblock show that the addition of salt has no effect on the aggregation number of the diblocks. At this point the nature of the core has to be discussed (the charged chains in the previous examples were all fully charged). Note that a variation of the aggregation number was observed for reputed glassy cores [6] or not observed for non-glassy cores (the present manuscript with PEP cores). Similar liquid-like cores of PEE of even longer extension, were found able to evolve in reference [14]. Then, we conclude that the core nature does not seem to prevent salt-induced changes although one cannot

prove that a true equilibrium is reached. Our intriguing observation about asymmetry may be fortuitous but new theoretical modeling may be needed anyhow to fully predict the aggregation numbers of charged diblock polymers.

3.2 Conformation of the corona of spherical polyelectrolyte brushes

The corona conformation was studied by neutron scattering using samples prepared with a mixture of H_2O and D_2O in such a way that only the $NaPSS_d$ groups are visible. An example of scattering curves obtained at a copolymer concentration of 0.5 wt% ($c/c^* \approx 0.25$) and at a NaCl concentration of 1 M, are shown in Figure 2. A quantitative analysis is performed by fitting the differential cross-sections to

$$\sigma(q) = \sigma_s P_s(q)\,, \tag{4}$$

where $P_s(q)$ is the form factor of the corona, σ_s the differential cross-section per unit volume of non-interacting coronae at $q = 0$:

$$\sigma_s = (c\rho/pM) b_s^2 N_s^2 p^2 \tag{5}$$

and b_s is the apparent contrast length of the $NaPSS_d$ monomer in the solvents, N_s is the degree of polymerization of $NaPSS_d$ moiety, and ρ is the solvent density. In previous work [16], it was shown that, for no added salt, the form factor of the corona can be described by the following expression:

$$P_s(q) = (1 - 1/p)\,|F_{ave}(q, R_m, R_c, \alpha)|^2 + (1/p) P_{ind}(q, R_m - R_c)\,. \tag{6}$$

The first term $(1-1/p)\,|F_{ave}(q, R_m, R_c, \alpha)|^2$ represents the scattering by the average profile of the monomers and $F_{ave}(q)$ is the normalized Fourier transform of the centrosymmetric density profile of the corona $\phi(r) \sim 1/r^\alpha$, with $\alpha = 3 - 1/\nu$ where ν is related to the chain statistics and then equal to 1 without salt ($\alpha = 2$). The second term $P_{ind}(q, R_m - R_c)$ is the form factor of a rod of length $R_m - R_c$, which approximates the scattering of the fluctuating profile by $(1/p)P_{ind}(q)$ which dominates at large scattering vectors. This modeling is of course approximate since the chains are not fully extended as confirmed by recent simulations [22], which show that the extension is only of the order of 60% of the contour length.

The α-values in equation (6) represent averages over the whole shell and are expected to lie in between 0 and 2, where the limiting values should be the collapsed state ($\nu = 1/3$) and the elongated state ($\nu = 1$) for which equation (6) holds.

When dealing with added-salt cases, a first approach is to restrict our analysis to low scattering vectors, where the fluctuating profile contribution is negligible in the scattering signal. For the whole salt concentration range investigated, we found that the fluctuating part has a little influence at low scattering vectors ($qR_m \leqslant 4$). In this q range, the absolute intensities were fitted to equation (6) without the fluctuating term, the two adjustable parameters being R_m and α. The values of R_m and α at different salinities are given in Table 1. Whatever is the exact meaning of α, a radius of gyration R_g of the whole micelle can be calculated from R_c, R_m and α-values following the expression (see App. A):

$$R_g^2 = R_c^2(3\beta/5) + R_m^2(1-\beta)[(3-\alpha)/(5-\alpha)] \times [1 - (R_c/R_m)^{5-\alpha}]/[1 - (R_c/R_m)^{3-\alpha}]\,, \tag{7}$$

where β (= 0.17) is the fraction of hydrophobic monomers in the diblock. In Table 1, we present the ratios R_g/R_m, which provide a measure of the micelle compactness. The validity of equation (7) has been checked by performing

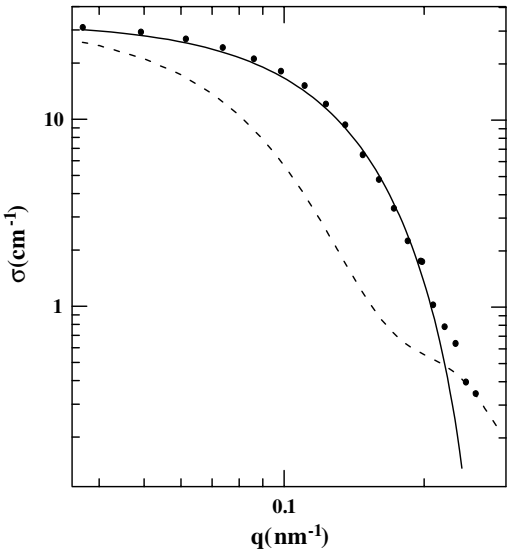

Fig. 2. Absolute intensity scattered by the coronae at small scattering vector q measured on dilute sample ($c = c^*/4$) at a NaCl concentration: $c_s = 1$ M. The signal (points) can be well described by expressions (4–6) neglecting the fluctuating part. The full line represents the best fit with $R_m = 20$ nm and $\alpha = 1.3$. For comparison the best fit of the data obtained without salt (dashed line) is reported: $R_m = 38$ nm and $\alpha = 2$.

Table 1. Salt concentration c_s, micelle radius R_m (±5%), exponent α (±15%) of the power law corona density, exponent ν related to the chain statistics, ratio of radius of gyration over the micelle radius R_g/R_m, and hydrodynamic radius R_h (±7%).

c_s (M)	R_m (nm)	α	ν	R_g/R_m	R_h (nm)
0	38	2	1	0.56	36
0.001	–	–	–	–	36
0.003	–	–	–	–	36
0.01	35	1.9	0.9	0.57	35
0.03	30	1.7	0.8	0.60	32
0.1	26	1.5	0.7	0.62	27
0.3	23	1.4	0.6	0.63	25
1	20	1.3	0.6	0.65	20
3	17	1.2	0.55	0.66	16

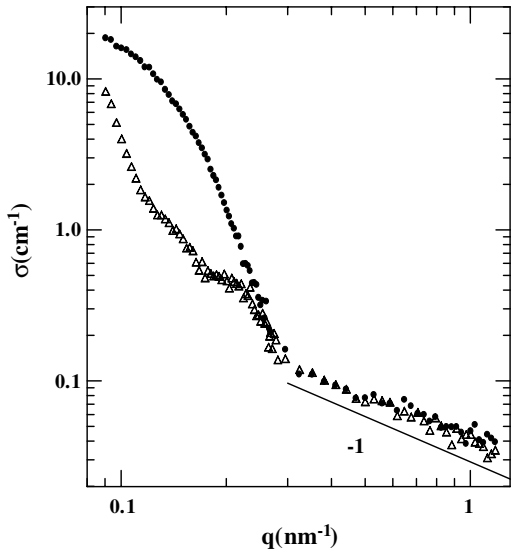

Fig. 3. Absolute intensities scattered by the coronae measured on dilute samples ($c = c^*/4$) at NaCl concentrations: $c_s = 1$ M (full points) and $c_s = 0$ M (open triangles). At high scattering vectors, a q^{-1}-dependence is observed whatever the salinity is.

intensity light scattering on a sample without salt, where it was found that $R_g = 25$ nm (typical errors on these measurements are of order 10%) which is in agreement with the value $R_g = 21$ nm obtained by equation (7) from neutron scattering experiments. The advantage of this treatment is that very low values of R_g can be determined whereas, from intensity light scattering measurements, only radii of gyration larger than about 20 nm can be measured. For comparison the hydrodynamic radii R_h measured by QLS are also collected in Table 1. Within the experimental error, the hydrodynamic radius of the micelle is identical to the radius of the whole micelle R_m deduced from neutron scattering in the salt concentration range 0 to 3 M. This experimental observation underscores that the hydrodynamic radius is a valid measure for the corona thickness, an identity currently assumed in the literature for comparison with scaling laws [23] but never checked to our knowledge. However, we are not aware of any calculation explaining this identity between R_h and R_m (see App. B).

As the salt concentration increases, the ratio R_g/R_m increases slightly from 0.56 up to 0.66 (0.77 is the value for a dense sphere). At high salinity ($c_s > 0.3$ M), the exponent α tends to a constant and the deduced exponent ν is close to an excluded-volume statistics ($\approx 3/5$).

To get more insight into the way a micelle contracts, it is interesting to examine the fluctuating part of the scattering profile at larger scattering vectors. Surprisingly, it is clear from the spectra that this part remains identical to the zero–added-salt spectrum (Fig. 3). This means that the chains remain rod-like at a small spatial scale in high salt (q^{-1}-dependence). The constancy of the absolute intensity at large q for zero and 1 M added-salt cases shows that one measures the mass per unit contour length in this range, a characteristic of rod-like chains like

Table 2. Hydrodynamic radii R_h (±7%) and core radii R_c (±4%) of copolymer micelles made of N_s sodium poly(styrenesulfonate) units and N_c poly(tertbutylstyrene) units having a degree of aggregation p in salt-free solutions. Dynamic light scattering and small-angle neutron scattering were used to characterize the structural properties of these micelles.

N_s	N_c	R_h (nm)	R_c (nm)	p
869	54	132	4.1	19
611	15	86	2.5	16
590	43	100	4.2	26
404	25	53	3.6	28
227	48[(a)]	38	5.5	85
211	13	42	2.8	26

([a]) Copolymer made of PEP units instead of poly(tertbutylstyrene) units.

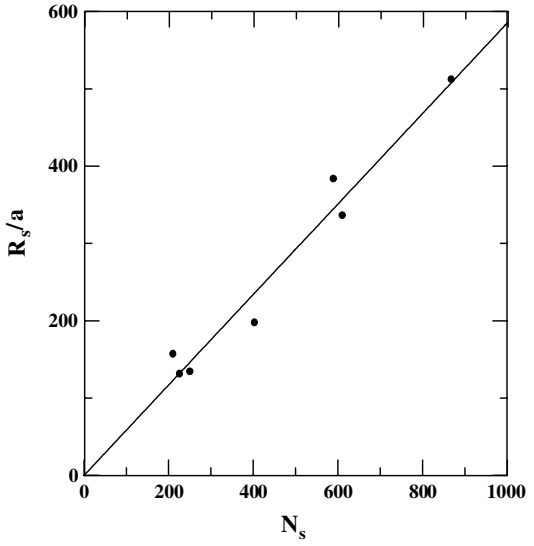

Fig. 4. Corona thickness ($R_s = R_h - R_c$) of micelles of copolymers with N_s sodium poly(styrenesulfonate) monomers of contour length a (= 0.25 nm) and N_c hydrophobic units in salt-free solutions (see Tab. 2). The full line is the best fit: $R_s/a = 0.58N_s$.

the worm-like chain [24]. This means that, though contracting, the charged shell remains rod-like at small scale and the chain can be viewed as a "surveyor's chain" which folds by rotating rigid segments of persistence length l_p. Of course this must be viewed as a qualitative picture since, for instance, l_p has no reason to stay constant along the radial distance from the core. However, this scenario appears to describe more precisely how a charged chain contracts than to merely infer from the $\nu = 3/5$ value that the conformation of the chain is identical to neutral flexible chains in good solvent when salted enough.

In salt-free solutions the extension of the corona is about 50% of the contour length of PSSNa chain ($N_s a = 251 \times 0.25$ nm) which is in close agreement with Monte Carlo simulation result $R_s = 0.6N_s a$ [22]. A systematic study, on a set of polyelectrolyte block copolymer micelles

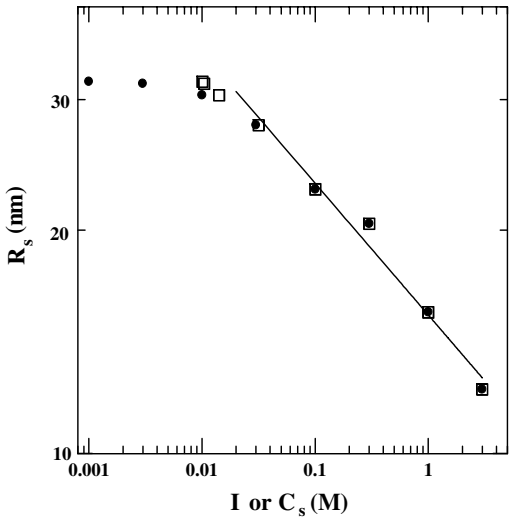

Fig. 5. Salt dependence of the micellar corona thickness. Empty squares and full points are R_s as a function of the ionic strength inside the corona (I) and of the concentration of the added salt (c_s), respectively.

(see Tab. 2 and Fig. 4), shows that this behavior is quite general. The salt dependence of the corona thickness of micelles, calculated as $R_s = R_h - R_c$, is shown in Figure 5. At the lowest salt concentrations, the thickness of the corona remains essentially constant and a significant contraction is observed above an added-salt concentration $c_s \approx 2\times10^{-2}$ M. This crossover should roughly correspond to the average ionic strength of the free counterions in the corona I_0 [4,6–8]. Following Donnan equilibrium, as derived by Hariharan *et al.* [7] the ionic strength, I, inside the corona is related to the added-salt concentration by

$$I = c_s(1 + (I_0/c_s)^2)^{1/2}\,. \tag{8}$$

Assuming that all the counterions are trapped inside the corona, as it is expected from Monte Carlo simulations [22,25], I_0 is given by

$$I_0 = pzN_s/2V_s\,, \tag{9}$$

where V_s is the volume of the corona ($\approx 4\pi(R_h^3 - R_c^3)/3$) and z the mean effective charge per monomer of the corona after a Manning condensation of a fraction of the counterions on the arms. The quantity z is equal to $a/(\lambda_B f)$ since this is the local rod-like structure of the chain which rules the condensation [22] with λ_B the Bjerrum length. Using the experimental values given above, one obtains $I_0 = 2.3\cdot10^{-2}$ M which is in agreement with the salt crossover concentration observed in Figure 5. Note that recent experiments [8,14] report lower threshold values suggesting that some overcondensation (reducing the free ions number) occurs for large densities of chains in the corona. One must also take into account uncertainties on I_0 which mostly come from uncertainties on aggregation numbers and brush extension. Moreover, the Donnan approximation assumes an homogeneous brush and I_0 is compared to a crossover value whose determination is rather imprecise.

A plot of R_s *versus* I, in Figure 5, shows that salt concentrations and internal ionic strengths coincide when c_s is larger than 10^{-2} M and yields a straight line in a log-log representation with a slope -0.18.

This finding is in agreement with results obtained on stable micelles made up of PS-PANa diblocks [13], where in presence of added KBr the outer radius contracts as $c_s^{-0.2}$. Similar weak decreases of the micelle size were already observed [5,6,14] but quantitative comparisons with these results are sometimes meaningless since the aggregation numbers vary upon addition of salt.

Let us now compare the variation of the corona thickness due to ionic strength with theoretical predictions for star-like brushes of radius R_s (here $R_c \ll R_s$) and planar brushes of layer thickness L_s. The polyelectolyte chain can be considered as a semi-flexible polymer chain with an electrostatic virial coefficient w related to the Debye screening length λ_D [26,27]. Despite an enormous interest in polyelectrolytes the l_p-dependence with added salt is not well established:

$$l_p \sim \lambda_D^x\,, \tag{10}$$

where x is equal to 2 following the Odijk-Skolnick-Fixman approach [28] or equal to 1 on the basis of the Barrat-Joanny prediction for flexible polyelectrolytes [29]. The layer thickness is obtained by equating the chain elasticity of the semi-rigid shell per unit volume $(pR_s^2/N_s l_p a)/R_s^3$ to the electrostatic excluded-volume interaction $w(pzaN_s/l_pR_s^3)^2$ for stars which gives

$$\begin{aligned} &R_s \cong az^{2/5}N_s^{3/5}p^{1/5}(w/l_pa^2)^{1/5} \qquad \text{and} \\ &L_s \cong az^{2/3}N_s(\Sigma w/l_p)^{1/3}\,, \end{aligned} \tag{11}$$

where Σ is the chain grafting density of a planar brush.

Whatever the exact variation of the electrostatic persistence length is with ionic strength, the curvature strongly decreases the sensitivity of polyelectrolyte brushes to added salt: the relative variation in the effective exponent should be 3/5 smaller in the spherical geometry than in the planar geometry. Following the Skolnick-Fixman calculation of the virial w for a semi-flexible chain, we adopt the scaling relation: $w \sim l_p^2\ \lambda_D$ which leads to $R_s \sim l_p^{1/5}\lambda_D^{1/5}$ in spherical geometry (interestingly enough, an isotropic virial [30] like $w \sim l_p^3$ would lead to the same conclusions). One then gets $R_s \sim c_s^{-(x+1)/10}$ suggesting that the value $x = 1$ is in better agreement with our experimental finding ($R_s \sim c_s^{-0.2}$). Previous measurements [12] of the thickness of a free-standing film made up of similar diblock copolymer lead to $L_s \sim c_s^{-(0.31\pm0.06)}$, also in agreement with an exponent $(x+1)/6$ with $x = 1$. Such a dependence $l_p \sim \lambda_D$ is compatible with several previous experimental observations [31] and is consistent with the behavior in salt-free conditions since a nice crossover is obtained in the limit of negligible added-salt concentration. When inserting $I_0 = pzN_s/R_s^3$ into expressions (10) and (11) with $x = 1$ one recovers the layer thicknesses for salt-free solutions [4,32]: $R_s \cong aN_sp^0z^{-1/2}$ and $L_s \cong aN_s\Sigma^0z^{-1/2}$ for the planar case.

A lower bound for the absolute value of the persistence length can be deduced in order to check the consistency of our scenario: if one assumes that a chain switches from a rod of about 3 nm at $c_s \sim 3 \cdot 10^{-2}$ M to a worm-like chain at $c_s \sim 3$ M, our model where $l_p \sim \lambda_D$ implies that $l_p(3\text{ M}) \sim 3$ nm. From Figure 3, the scattered signal follows a q^{-1}-dependence on q-values such as $ql_p > 1$ in agreement with reference [24]. A direct determination of l_p from the spectra is not reliable enough because of the superimposition of the average profile at low wave vectors. However, our indirect estimation of l_p seems in good agreement with recent determinations for linear NaPSS polyelectrolytes [33].

4 Conclusion

In this work we have studied the inner structure of spherical charged brushes formed by neutral-charged copolymers as a function of added NaCl salt concentration. It has been shown that added salt has no influence on the aggregation number p of the micelles for the kind of asymmetric polymer used whilst more precise studies are needed to judge whether or not asymmetry is a key parameter. The study of the spherical polyelectrolyte corona (spherical brush) has demonstrated that a measure of the hydrodynamic radius provides a true measurement of the corona size. More work is also needed to fully understand the reason of this equivalence quite often postulated without justification. We have shown that while contracting above some threshold in salt as expected, a spherical polyelectrolyte brush does not exactly reach a flexible neutral brush state in high salt [32]. Due to its large persistence length even in high salt (where l_p is typically of order ten monomers), the chain contracts more like a worm-like chain whose persistence length decreases with salt (proportional to the Debye screening length in this case), maybe like a "surveyor's chain".

One of us (FM) thanks the Région Charentes-Poitou for partial support. J.W.M. acknowledges support of the National Science Foundation, CTS and DMR programs, Grant NSF-CTS-9616797, and of the Division of Chemical Scences, Geosciences, and Biosciences, Office of Basic Energy Sciences, U.S. Department of Energy, under contract No. DE-AC05-00OR22725 with Oak Ridge National Laboratory, managed and operated by UT-Battelle, LLC. We sincerely thank L. Belloni and M. Roger for fruitful discussions, shared calculations and advices.

Appendix A.

The structure of the micelle of whole radius R_m is that of a dense hydrophobic spherical core of radius R_c surrounded by a shell of charged polymer chains. The whole radius of gyration of the micelle can be written as

$$R_g^2 = \beta R_{gcore}^2 + (1-\beta) R_{gshell}^2 , \qquad (A.1)$$

where β is the fraction of hydrophobic monomers in the diblock. The radius of gyration of the core is

$$R_{gcore}^2 = (3/5) R_c^2 . \qquad (A.2)$$

If the shell has an average density profile $\phi(r) \sim 1/r^\alpha$, then

$$R_{gshell}^2 = \int_{R_c}^{R_m} r^{4-\alpha} \mathrm{d}r \Big/ \int_{R_c}^{R_m} r^{2-\alpha} \mathrm{d}r . \qquad (A.3)$$

After integration, this leads to

$$R_{gshell}^2 = R_m^2 [(3-\alpha)/(5-\alpha)] \times [1-(R_c/R_m)^{5-\alpha}]/[1-(R_c/R_m)^{3-\alpha}] . \qquad (A.4)$$

Appendix B.

The hydrodynamic radius R_h of a neutral star having p arms with N monomers can be calculated using the configurational preaveraging Kirkwood-Riseman approximation [34]

$$1/R_h = (pNa)^{-1} + (pN)^{-2} \sum_{i,j=1}^{pN} \langle r_{ij}^{-1} \rangle (1-\delta_{ij}) . \qquad (B.1)$$

In this expression, it is assumed that the size of the monomer, a, is larger than the size of solvent molecules and smaller than the distance r_{ij} between monomers i and j. For a large number of monomers hydrodynamics interactions are dominant and

$$1/R_h = (pN)^{-2} \sum_{i,j=1}^{pN} \langle r_{ij}^{-1} \rangle (1-\delta_{ij}) . \qquad (B.2)$$

This quantity is related to the form factor $P(q) = (pN)^{-2} \sum_{i,j=1}^{pN} \langle (qr_{ij})^{-1} \sin(qr_{ij}) \rangle$ as follows:

$$1/R_h = 2/\pi \int_0^\infty P(q) \mathrm{d}q , \qquad \text{when } pN \gg 1 . \qquad (B.3)$$

A good approximation for the form factor is $P(q) \approx F^2(q)$, where $F(q)$ is the normalized Fourier transform of the centrosymmetric density profile of the star $\phi(r)$. Assuming that $\phi(r) \sim 1/r^{(3-1/\nu)}$, where ν is related to the chain statistics of the arms, after some algebric manipulations, we obtain

$$R_h/R_m = 1 - \nu/2 , \qquad (B.4)$$

where R_m is the overall radius of the star.

This result can be reasonably extended to charged copolymer micelles having a small core as it is the case with the system studied. In salt-free conditions, within the framework developed above, we expect that $R_h/R_m = 1/2$, which is far from the experimental

value $R_h/R_m \approx 1$. In order to check the validity of the approximations done to get expression (B.4) we have computed R_h using directly equation (B.2) and a Monte Carlo simulation to generate the structure of a "charged star" of 54 arms and 251 monomers per arm [22]. The value obtained is R_h/R_m is also close to 1/2 as derived from the analytical calculations.

More theoretical work is needed to fully describe the hydrodynamic radius of such a star and in particular what is the exact screening coupled to electrostatic interactions. In the prior calculation, it is implicitely assumed that the solvent can freely penetrate into the whole star. This hypothesis is reasonable when the compactness of the star is low but less and less correct as the compactness increases. If the star is fully compact then the solvent prefers to circumvent the star and R_h should be equal to R_m. A reasonable assumption is that the compactness of our micelles is high enough to reach this latter limit.

References

1. U. Raviv, S. Giasson, N. Kampf, J.F. Gohy, R. Jérôme, J. Klein, Nature **425**, 163 (2003).
2. A. Albersdörfer, E. Sackmann, Eur. Phys. J. B **10**, 663 (1999).
3. A. Constancis, R. Meyrueix, N. Bryson, S. Huille, J.M. Grosselin, T. Gulik-Krzywicki, G. Soula, J. Colloid Interface Sci. **217**, 357 (1999).
4. P. Pincus, Macromolecules **24**, 2912 (1991).
5. J.W. Mays, Polym. Commun. **31**, 170 (1990).
6. P. Guenoun, H.T. Davis, J.W. Mays, M. Tirrell, Macromolecules **29**, 3965 (1996).
7. R. Hariharan, C. Biver, J.W. Mays, W.B. Russel, Macromolecules **31**, 7506 (1998).
8. M. Balastre, F. Li, P. Schorr, J. Yang, J.W. Mays, M.V. Tirrell, Macromolecules **35**, 9480 (2002).
9. P. Guenoun, F. Muller, M. Delsanti, L. Auvray, Y.J. Chen, J.W. Mays, M. Tirrell, Phys. Rev. Lett. **81**, 3872 (1998).
10. O.V. Borisov, E.B. Zhulina, Eur. Phys. J. B **4**, 205 (1998).
11. N. Dan, M. Tirrell, Macromolecules **28**, 4310 (1993).
12. P. Guenoun, A. Schalchli, D. Sentenac, J.W. Mays, J.J. Benattar, Phys. Rev. Lett. **74**, 3628 (1995).
13. J.R.C. van der Maarel, W. Groenewegen, S.U. Egelhaaf, A. Lapp, Langmuir **16**, 7510 (2000).
14. S. Förster, N. Hermsdorf, C. Böttcher, P. Lindner, Macromolecules **35**, 4096 (2002).
15. P.L. Valint, J. Bock, Macromolecules **21**, 175 (1988).
16. F. Muller, M. Delsanti, L. Auvray, J. Yang, Y.J. Chen, J. Mays, B. Demé, M. Tirrell, P. Guenoun, Eur. Phys. J. E **3**, 45 (2000).
17. `http://www-llb.cea.fr/`.
18. `http://www.ill.fr`.
19. F. Muller, PhD Thesis, Université La Rochelle, available at `http://www.drecam.cea.fr/articles/s00/124/`.
20. See, for instance, B. Chu, *Laser Light Scattering*, second edition (Academic Press, Inc. New York, 1991).
21. P. Guenoun, M. Delsanti, D. Gazeau, L. Auvray, D.C. Cook, J.W. Mays, M. Tirrell, Eur. Phys. J. B **1**, 77 (1998).
22. M. Roger, P. Guenoun, F. Muller, L. Belloni, M. Delsanti, Eur. Phys. J. E **9**, 313 (2002).
23. See, for instance, R.D. Wesley, T. Cosgrove, L. Thompson, S.P. Armes, N.C. Billingham, F.L. Baines, Langmuir **16**, 4467 (2000); C. Burguière, C. Chassenieux, B. Charleux, Polymer **44**, 509 (2003).
24. J. des Cloizeaux, Macromolecules **6**, 403 (1973).
25. L. Belloni *et al.*, J. Chem. Phys. **119**, 7560 (2003).
26. J.L. Barrat, J.F. Joanny, Adv Chem. Phys. **94**, 1 (1996).
27. T. Odijk, A.C. Houwaart, J. Polym. Sci. **16**, 627 (1978).
28. T. Odijk, J. Polym. Sci. **15**, 477 (1977); J. Skolnick, M. Fixman, Macromolecules **10**, 944 (1977).
29. J.L. Barrat, J.F. Joanny, Europhys. Lett. **24**, 333 (1993).
30. J.F. Argillier, M. Tirrell, Theor. Chim. Acta **82**, 343 (1992).
31. M. Tricot, Macromolecules **17**, 1698 (1984); W.F. Reed, S. Ghosh, G. Medjahdi, J. François, Macromolecules **24**, 6189 (1991).
32. O.V. Borisov, E.B. Zhulina, Macromolecules **35**, 4472 (2002).
33. E. Dubois, F. Boué, Macromolecules **34**, 3684 (2001).
34. J.G. Kirkwood, J.J. Riseman, J. Chem. Phys. **16**, 565 (1948).